



Short communication

Fabrication of LiCoO₂/helical nanocarbon composites and their effect on lithium cell performance

Toshiro Hirai^{a,*}, Toshihiro Yoshida^a, Yusuke Uno^{a,1}, Tomonobu Tsujikawa^b^a Department of Mechanical Systems Engineering, Toyama Prefectural University, Imizu-shi, Toyama-ken 939-0398, Japan^b NTT Facilities, Inc., Toshima-ku, Tokyo 170-0004, Japan

ARTICLE INFO

Article history:

Received 3 October 2010

Received in revised form 31 October 2010

Accepted 3 November 2010

Available online 12 November 2010

Keywords:

Lithium-ion cell

Cathode active material

Nanocarbon

Composite

Chemical vapor deposition

ABSTRACT

We fabricate LiCoO₂/helical nanocarbon (HCN) composites by forming HCNs on LiCoO₂ on which iron oxides (Fe₂O₃ or Fe₃O₄) are dispersed (LiCoO₂(Fe₂O₃) or LiCoO₂(Fe₃O₄)) as catalysts for HCN formation, and estimate their electrochemical properties. Granular nanocarbons form on LiCoO₂(Fe₂O₃) and LiCoO₂(Fe₃O₄) at 350 °C although HCNs of about 100 nm in diameter form on LiCoO₂(Fe₂O₃) at 450 °C. Transmission electron microscopy and energy dispersive X-ray spectroscopy measurements show that HCNs consist of stacked graphene layers for LiCoO₂(Fe₂O₃)/HCN composites fabricated at 450 °C. On the other hand, several-nm-thick tetragonal layer exists on the LiCoO₂ substrate and amorphous nanocarbons form on the tetragonal layer for LiCoO₂(Fe₂O₃)/HCN and LiCoO₂(Fe₃O₄)/HCN composites fabricated at 350 °C. X-ray diffraction measurements suggest that Fe₂O₃ and Fe₃O₄ do not completely inhibit LiCoO₂ decomposition. Cathodes containing LiCoO₂(Fe₂O₃)/HCN or LiCoO₂(Fe₃O₄)/HCN fabricated at 350 °C improve rate capability of lithium cells. However, this rate capability is not better than that of cathodes containing a mixture of LiCoO₂ and acetylene black.

© 2010 Elsevier B.V. All rights reserved.

1. Introduction

High-rate and long-life lithium-ion batteries have long been expected as automotive and next-generation industrial batteries. Cathode active material/carbon composites have been studied as means of prolonging cycle life of such batteries [1,2] as well as cathode active materials have been studied to improve lithium-ion cell capacity and rate capability [3–7].

On the other hand, some researchers have fabricated nanocarbons using chemical vapor deposition (CVD) [8–11]. Nanocarbons produced using CVD have a helical shape and are reported to be semimetals with the potential to be superconductive materials [12]. This suggests that they have high potential for use as conductive materials for the cathodes of lithium-ion cells. We have fabricated LiCoO₂/helical nanocarbon (HCN) composites and evaluated their electrochemical properties [13]. We successfully obtained composites from HCNs formed on a LiCoO₂ substrate. However, LiCoO₂ severely decomposed and a cell containing LiCoO₂/HCN composite exhibited a low specific capacity.

We used Fe₂O₃ and Fe₃O₄ as catalysts to fabricate LiCoO₂/HCNs effectively without LiCoO₂ decomposition at lower temperature to show better performance as cathode active material. We prepared a LiCoO₂ substrate on which iron oxides (Fe₂O₃ or Fe₃O₄) were dispersed (LiCoO₂(Fe₂O₃) or LiCoO₂(Fe₃O₄)) as catalysts for HCN formation. We then formed HCNs on LiCoO₂(Fe₂O₃) or LiCoO₂(Fe₃O₄) at 450 °C or lower and estimated effect of the composites on lithium cell performance.

2. Experimental

We used LiCoO₂ (Nippon Chemical Industrial Co., diameter: 10 μm) as a substrate and Fe₂O₃ and Fe₃O₄ (Wako Pure Chemical Industries, Ltd.) as catalysts for helical nanocarbon (HCN) formation using chemical vapor deposition (CVD).

We prepared slurries by dispersing 10 g of LiCoO₂ and 0.5 g of Fe₂O₃ or Fe₃O₄ into 50 ml of distilled water to uniformly and effectively disperse Fe₂O₃ or Fe₃O₄ on the surface of LiCoO₂ particles and stirred the solution containing the mixture in a beaker overnight on a hot plate at about 80 °C to evaporate water. The mixture was then dried overnight in vacuum at 80 °C.

We fabricated the composites by forming HCNs on the surface of LiCoO₂/Fe₂O₃ or LiCoO₂/Fe₃O₄ powder mounted on a ceramic boat using CVD in a quartz tube and supplied 60 ml min⁻¹ of C₂H₂ gas as a carbon source and 50 ml min⁻¹ of Ar as a carrier at 450 °C or 350 °C for 10 min.

* Corresponding author. Present address: SACI, Kyoto University, Nishikyo-ku, Kyoto 615-8520, Japan. Tel.: +81 75 383 3052; fax: +81 75 383 3048.

E-mail address: t-hirai@saci.kyoto-u.ac.jp (T. Hirai).

¹ Present address: Chuo Branch, NTT Facilities, Inc., Minato-ku, Tokyo 108-0023, Japan.

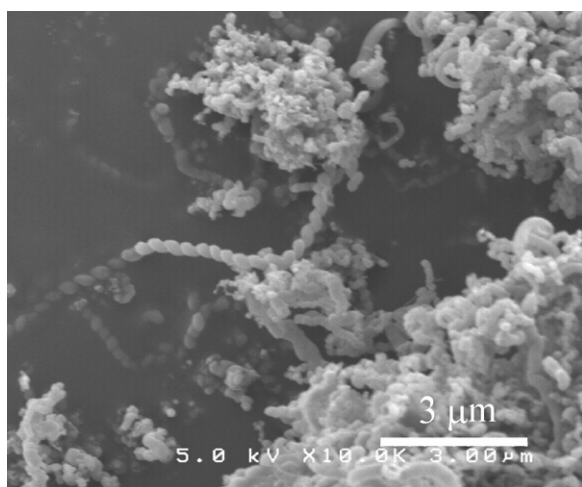


Fig. 1. SEM image of LiCoO₂/HCN composites fabricated at 450 °C for 10 min.

We estimated the electrochemical properties of the composites using a lithium cell. We fabricated cathode disks (area, 1.33 cm²) by mixing the obtained composites, acetylene black (AB, Denki Kagaku Kogyo Co.) and PTFE powder with a ratio of 70 wt% of LiCoO₂, 25 wt% of AB and HCNs formed using CVD, and 5 wt% of PTFE, and rolling the mixture into a flat sheet. We fabricated CR2032 coin-type cells for evaluating electrochemical properties. Each coin-type cell consisted of a cathode, a lithium anode (Honjo Chemical Co., area, 1.13 cm²) and a 1 M LiPF₆-ethylene carbonate/dimethyl carbonate (volume ratio: 1/1) electrolyte (Tomiyama Pure Chemicals Co.). Test cells were charged at 0.75 mA cm⁻² to 4.3 V and then discharged at constant current to 3.0 V at 21 °C after a 10-min rest.

3. Results and discussion

Fig. 1 shows a scanning electron microscope (SEM) image of the LiCoO₂/HCN composite. HCNs are formed on the LiCoO₂ surface. However, the HCNs are not distributed uniformly and the bare LiCoO₂ surface can be seen. HCNs have a helical shape with a diameter of 200 nm or smaller. We generally observed HCNs with an irregular helical shape. We have not found an optimum fabrication condition of HCNs with a regular helical shape.

Fig. 2 shows transmission electron microscope (TEM) photos of the composites fabricated from HCNs formed on LiCoO₂ substrate without iron oxides at 450 °C. HCNs contain many crystalline boundaries of graphene layers and serious turbulence was also observed, indicated with the circle in Fig. 2, which may result in an irregular helical shape of HCNs. We measured contents of the composites by energy dispersive X-ray spectroscopy (EDS). Fig. 3 shows areas for EDS measurements as squares. The results are listed in Table 1. Carbon mainly existed in dark areas 1, 2, 3, and 4 around the white area. On the other hand, white area 5 contained more than 60% Co, which is larger than the Co percentage of LiCoO₂. This suggests that area 5 contained Co and CoO formed from decomposed LiCoO₂.

Table 1
Results of EDS measurements.

Area	Amount of atoms (%)				Total
	C	O	Co		
1	99.52	0.41	0.06		100.00
2	99.04	0.74	0.22		100.00
3	89.96	5.94	4.10		100.00
4	99.64	0.28	0.09		100.00
5	25.92	11.27	62.80		100.00

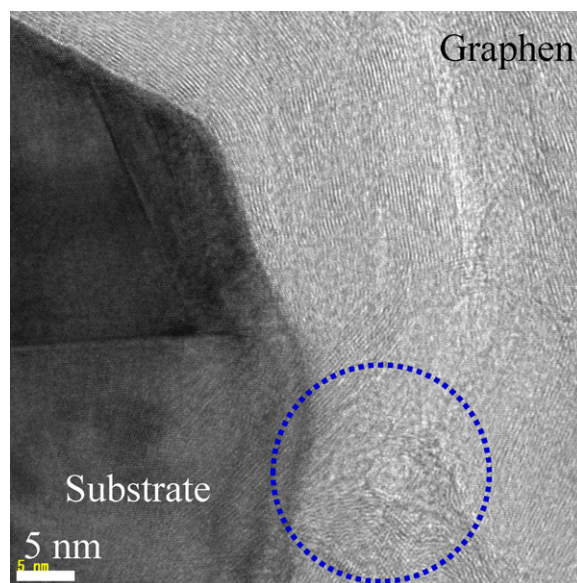


Fig. 2. TEM image of LiCoO₂/HCN composite fabricated at 450 °C for 10 min.

Furthermore, we used X-ray diffraction (XRD) to estimate the stability of LiCoO₂ under our experimental conditions. Fig. 4 shows XRD patterns of LiCoO₂/HCN composites fabricated at 450 °C. The XRD contains peaks of Li₂CO₃, Co, and CoO and no peaks of LiCoO₂, which shows that LiCoO₂ decomposed without iron oxides. The results coincide with those of EDS measurements.

We then fabricated a composite from HCNs formed on LiCoO₂ substrate with Fe₂O₃ or Fe₃O₄ and estimate its effect on inhibition of LiCoO₂ decomposition. Fig. 5 shows SEM photos of the composite fabricated with Fe₂O₃ at 450 °C. HCNs were successfully formed on LiCoO₂ particles and there was no significant difference in the HCN formation from the composites fabricated without iron oxides. We obtained the same results for the composite fabricated with Fe₃O₄. On the other hand, we observed nanocarbons were not helical shaped for the composites fabricated at 350 °C (Fig. 6). “Immature” and particulate HCNs formed on the substrate at 350 °C.

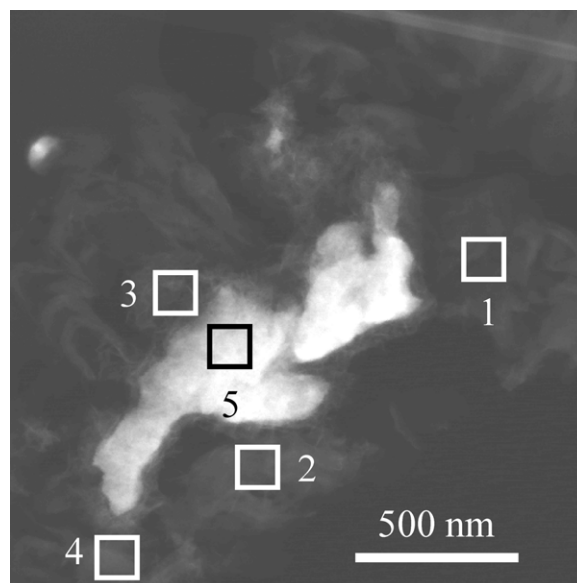


Fig. 3. TEM image of LiCoO₂/HCN composite fabricated at 450 °C for 10 min, and areas for EDS measurements.

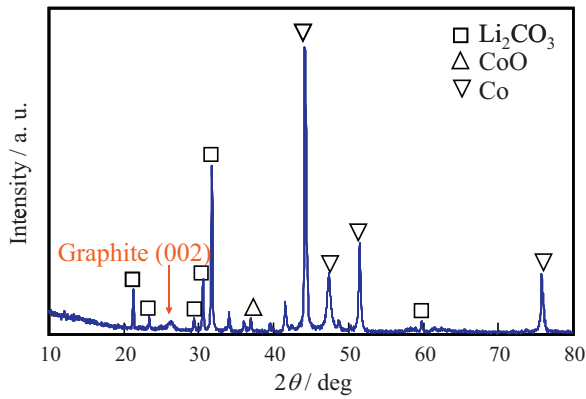


Fig. 4. XRD patterns of LiCo₂/HCN (450 °C).

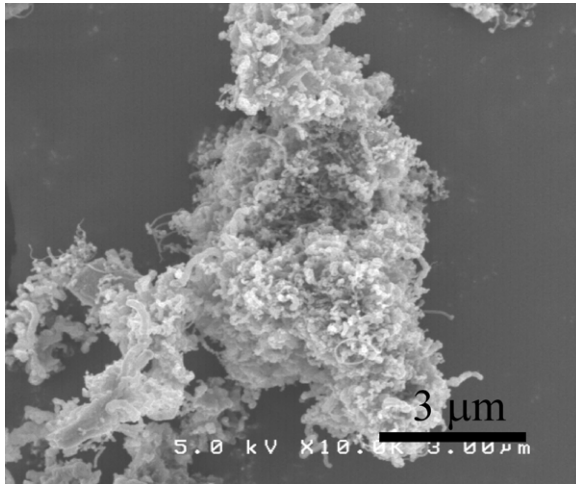


Fig. 5. SEM photo of LiCo₂(Fe₂O₃)/HCN fabricated at 450 °C.

Fig. 7 shows TEM photos of the composite fabricated with Fe₂O₃ at 350 °C. Fig. 7(a) shows TEM image of the area where there was Fe₂O₃, and Fig. 7(b) shows TEM image of the area where there was no Fe₂O₃.

By fabricating at 350 °C, amorphous nanocarbons (C in Fig. 7), formed on the LiCo₂ substrate (A in Fig. 7), and there was no significant difference in shape due to the existence of Fe₂O₃. We also observed a tetragonal thin layer (B in Fig. 7) on the substrate A. Fig. 8 shows TEM photos of the composite fabricated with Fe₃O₄ at

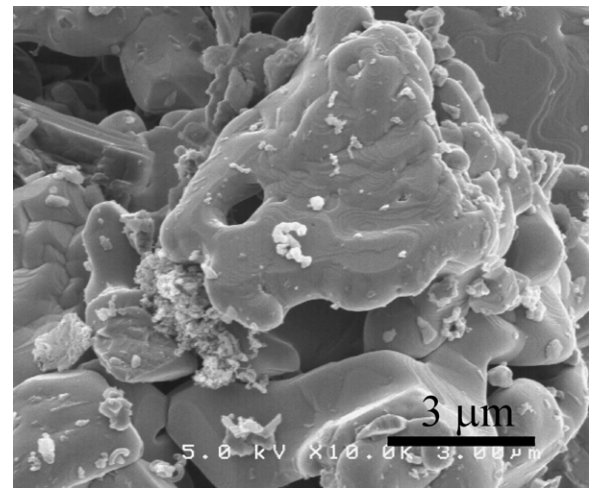


Fig. 6. SEM photo of LiCo₂(Fe₂O₃)/nanocarbon fabricated at 350 °C.

Table 2

XRD peak intensity ratio for LiCo₂/nanocarbon composites.

Composite	A/B	A/C	A/D
LiCo ₂ (Fe ₂ O ₃)/HCN (350 °C)	10.37	335.8	386.7
LiCo ₂ (Fe ₂ O ₃)/HCN (450 °C)	11.86	4.123	17.34
LiCo ₂ /HCN (450 °C)	1.984	1.051	0.0313

350 °C. We observed the same condition for the composite fabricated with Fe₃O₄ at 350 °C shown in both of Fig. 8(a) and (b) as that for the composite fabricated with Fe₂O₃ at 350 °C.

We observed a tetragonal layer on as-received LiCo₂ particles. We therefore do not conclude that this layer formed using CVD. Kobayashi et al. reported a layer on Li(NiCo)O₂ [14], which corresponds to what we observed.

Fig. 9 shows XRD patterns of LiCo₂/nanocarbon composites prepared with and without Fe₂O₃, LiCo₂(Fe₂O₃)/HCN (350 °C), LiCo₂(Fe₂O₃)/HCN (450 °C), and LiCo₂/HCN (450 °C). The XRD patterns indicate that LiCo₂ retained its original structure in part but it also suggests that addition of Fe₂O₃ did not prevent LiCo₂ from decomposing.

We also measured XRD for LiCo₂(Fe₃O₄)/HCN composite fabricated at 350 °C and confirmed addition of Fe₃O₄ inhibited LiCo₂ decomposition through HCN fabrication.

We evaluated LiCo₂ decomposition in relation to the addition of Fe₂O₃ and HCN fabrication temperature. Table 2 shows intensity

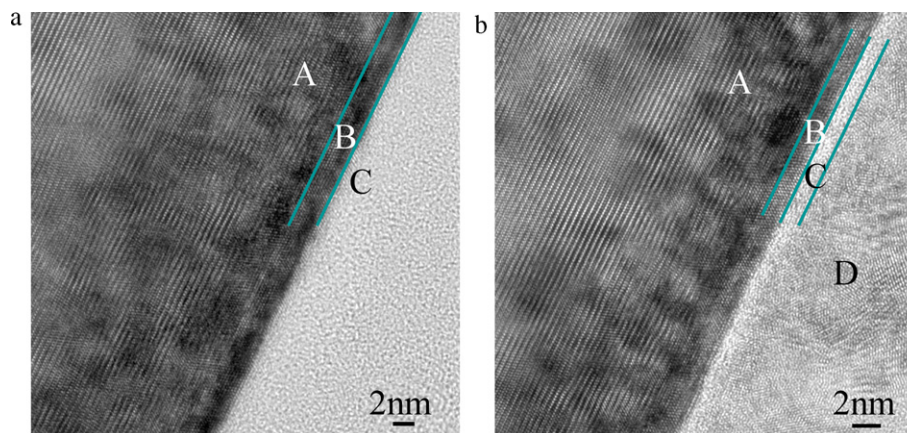


Fig. 7. TEM images of LiCo₂(Fe₂O₃)/nanocarbon composites fabricated at 350 °C for 10 min. (A) LiCo₂ substrate, (B) tetragonal layer, (C) nanocarbon fabricated using CVD, and (D) deposited Ti layer for TEM measurements.

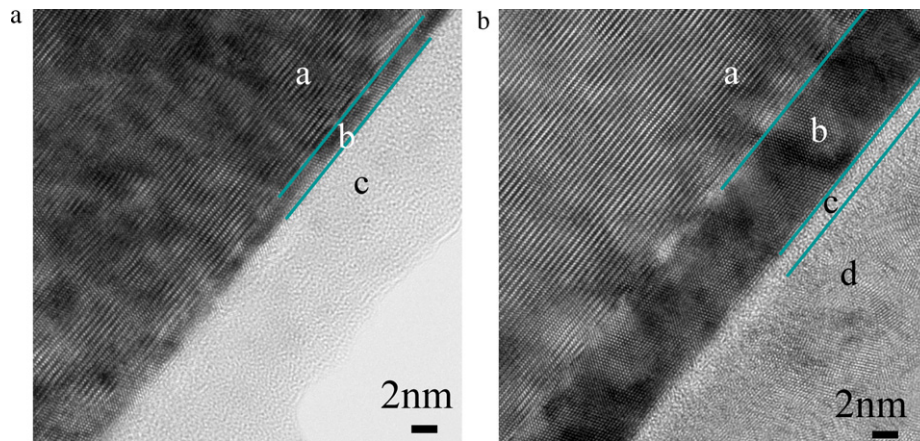


Fig. 8. TEM images of $\text{LiCoO}_2(\text{Fe}_3\text{O}_4)/\text{nanocarbon}$ composites fabricated at 350°C for 10 min. (A) LiCoO_2 substrate, (B) tetragonal layer, (C) nanocarbon fabricated by CVD, and (D) deposited Ti layer for TEM measurements.

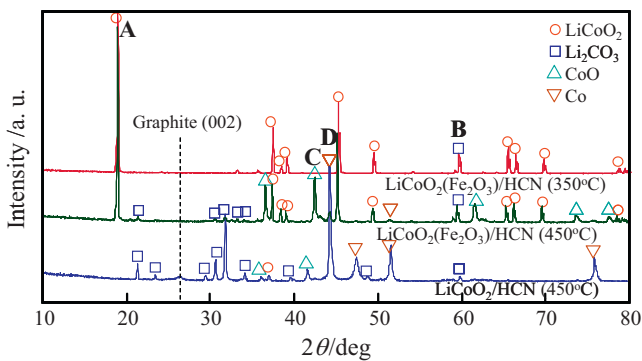


Fig. 9. XRD patterns of $\text{LiCoO}_2/\text{nanocarbon}$ composites fabricated with and without Fe_2O_3 .

ratios of main peaks of Li_2CO_3 (peak B in Fig. 9), CoO (peak C in Fig. 9), and Co (peak D in Fig. 9) based on LiCoO_2 peak (peak A in Fig. 9). XRD peak intensity ratios indicate that LiCoO_2 decomposition was significantly inhibited by coating with Fe_2O_3 and that HCN fabrication temperature decreased.

We estimated the electrochemical properties of $\text{LiCoO}_2/\text{nanocarbon}$ composites using a lithium cell. Fig. 10 shows rate capability of lithium cells containing $\text{LiCoO}_2(\text{Fe}_2\text{O}_3)/\text{HCN}$ composites, $\text{LiCoO}_2(\text{Fe}_2\text{O}_3)/\text{HCN}$ (350°C) and $\text{LiCoO}_2(\text{Fe}_2\text{O}_3)/\text{HCN}$ (450°C), compared with that of a lithium cell containing as-received LiCoO_2 . The cell containing $\text{LiCoO}_2(\text{Fe}_2\text{O}_3)/\text{HCN}$ (350°C) showed better rate

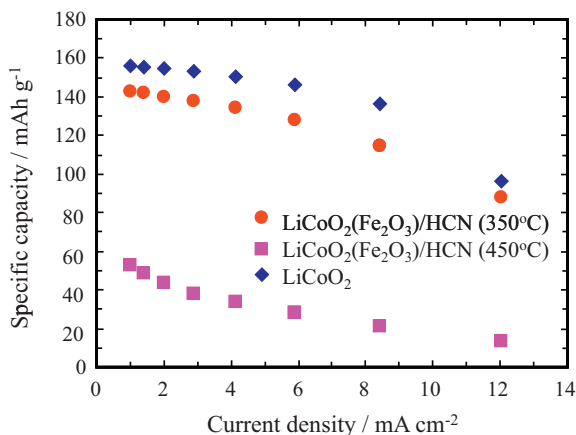


Fig. 10. Rate capability of lithium cells containing $\text{LiCoO}_2(\text{Fe}_2\text{O}_3)/\text{HCN}$ composite and cell containing as-received LiCoO_2 .

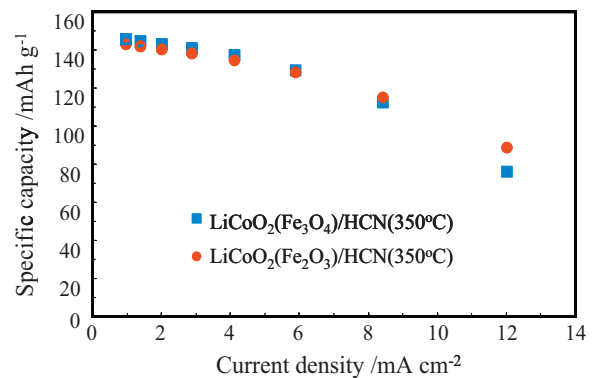


Fig. 11. Rate capability of lithium cells containing $\text{LiCoO}_2(\text{Fe}_2\text{O}_3)/\text{HCN}$ and $\text{LiCoO}_2(\text{Fe}_3\text{O}_4)/\text{HCN}$ composites fabricated at 350°C .

capability than cell containing $\text{LiCoO}_2(\text{Fe}_2\text{O}_3)/\text{HCN}$ (450°C). However, the rate capability of our composites is currently inferior to that of as-received LiCoO_2 . We also estimated the rate capability of a lithium cell containing $\text{LiCoO}_2(\text{Fe}_3\text{O}_4)/\text{HCN}$ composite (350°C). The results are shown in Fig. 11. The $\text{LiCoO}_2(\text{Fe}_3\text{O}_4)/\text{HCN}$ (350°C) cell showed the same rate capability as the $\text{LiCoO}_2(\text{Fe}_2\text{O}_3)/\text{HCN}$ (350°C) cell. By using iron oxide catalysts and fabricating the composites at lower temperature, LiCoO_2 decomposed less and the composites showed better cell performance than that of composites fabricated without the catalysts at higher temperature. The challenge is to fabricate composites with more crystallized HCN for better rate capability of lithium cells than that of the cathode mixed with LiCoO_2 and AB.

4. Conclusion

We fabricated $\text{LiCoO}_2/\text{helical nanocarbon}$ (HCN) composites by forming HCNs on LiCoO_2 on which iron oxides (Fe_2O_3 or Fe_3O_4) were dispersed ($\text{LiCoO}_2(\text{Fe}_2\text{O}_3)$ or $\text{LiCoO}_2(\text{Fe}_3\text{O}_4)$) as catalysts for HCN formation, and estimated their electrochemical properties.

Cathode active material/nanocarbon composites were fabricated by forming HCNs on LiCoO_2 coated with iron oxides (Fe_2O_3 or Fe_3O_4) to inhibit LiCoO_2 degradation. The following results were obtained: Granular nanocarbons were generated on LiCoO_2 with Fe_2O_3 and LiCoO_2 with Fe_3O_4 at 350°C although HCNs with about 100 nm diameter were generated on LiCoO_2 with Fe_2O_3 at 450°C . TEM measurements showed that HCNs consisted of stacked graphene layers for $\text{LiCoO}_2/\text{HCN}$ fabricated at 450°C . On the other hand, several-nm-thick tetragonal layer existed on the LiCoO_2

and amorphous nanocarbons formed on the tetragonal layer for $\text{LiCoO}_2(\text{Fe}_2\text{O}_3)/\text{HCN}$ and $\text{LiCoO}_2(\text{Fe}_3\text{O}_4)/\text{HCN}$ composites fabricated at 350°C . XRD measurements suggested that Fe_2O_3 and Fe_3O_4 did not completely inhibit LiCoO_2 decomposition. Cathodes containing $\text{LiCoO}_2(\text{Fe}_2\text{O}_3)/\text{HCN}$ or $\text{LiCoO}_2(\text{Fe}_3\text{O}_4)/\text{HCN}$ composites fabricated at 350°C improved rate capability, but this capability is not as good as that of cathodes containing a mixture of LiCoO_2 and AB.

Acknowledgment

The authors thank Nippon Chemical Industrial, Co. Ltd. for providing cathode active materials.

References

- [1] H. Huang, S.-C. Yin, L.F. Nazar, *Electrochem. Solid-State Lett.* 4 (2001) A170.
- [2] M. Tabuchi, Y. Nabeshima, K. Ado, T. Takeuchi, M. Shikano, H. Kageyama, K. Tatsumi, Extended Abstract for the 47th Battery Symposium in Japan, Tokyo, 2D19, 2006, pp. 362–363 (in Japanese).
- [3] T. Ohzuku, Y. Makimura, *Chem. Lett.* 30 (2001) 642.
- [4] A.K. Padhi, K.S. Nanjundaswamy, J.B. Goodenough, *J. Electrochem. Soc.* 144 (1997) 1188.
- [5] K. Amine, H. Yasuda, M. Yamachi, *Electrochem. Solid-State Lett.* 3 (2000) 178.
- [6] A. Yamada, S.C. Chung, K. Hinokuma, *J. Electrochem. Soc.* 148 (2001) A224.
- [7] A.S. Andersson, J.O. Thomas, B. Kalsa, L. Haggstroem, *Electrochem. Solid-State Lett.* 3 (2000) 66.
- [8] R.T.K. Baker, J.J. Chludzinski Jr., *J. Catal.* 64 (1980) 464.
- [9] S. Amelinckx, X.B. Zhang, D. Bernaerts, X.F. Zhang, V. Ivanov, J.B. Nagy, *Science* 265 (1994) 635.
- [10] M. Zhang, Y. Nakayama, L. Pan, *Jpn. J. Appl. Phys.* 39 (2000) L1242.
- [11] L. Pan, M. Zhang, Y. Nakayama, *Jpn. J. Appl. Phys.* 91 (2002) 10058.
- [12] K. Akagi, R. Tamura, M. Tsukada, *Phys. Rev. Lett.* 74 (1995) 2307.
- [13] Y. Uno, T. Tsujikawa, T. Hirai, *J. Power Sources* 195 (2010) 354.
- [14] H. Kobayashi, M. Shikano, S. Koike, H. Sakaebe, K. Tatsumi, *J. Power Sources* 174 (2007) 380.